

Implications of the new CDF II W -boson mass on two-Higgs-doublet models

Yang Hwan Ahn,^{*} Sin Kyu Kang,[†] and Raymundo Ramos[‡]

*School of Liberal Arts, Seoul National University of Science and Technology,
232 Gongneung-ro, Nowon-gu, Seoul 01811, Korea*

 (Received 25 May 2022; accepted 15 September 2022; published 26 September 2022)

We present the implications of the recent measurement of W boson at CDF II on the two-Higgs-doublet model (2HDM). In the analysis, we impose theoretical bounds such as vacuum stability and perturbative unitarity, and several experimental constraints. In addition, we take into account the measurement of $\sin^2\theta_W(m_Z)_{\overline{\text{MS}}}$ on top of the CDF W -boson mass to investigate how the S and T parameters are determined. We explore two possible scenarios depending on whether the Higgs boson observed at the LHC is the lighter or heavier of CP -even neutral Higgs bosons for 2HDM type I and II. Using the results, we show how the parameter space is constrained, and compare it with the one based on the PDG average of m_W . Furthermore, we explore phenomenological consequences of electroweak precision observables that can be affected by m_W within the predictions of the 2HDM, and the reduction in parameter space expected from future measurements at the Future Circular Lepton Collider.

DOI: [10.1103/PhysRevD.106.055038](https://doi.org/10.1103/PhysRevD.106.055038)

I. INTRODUCTION

Very recently, CDF announced a measurement of the W boson mass [1]

$$m_W^{\text{CDF}} = 80.4335 \pm 0.0094 \text{ GeV}. \quad (1)$$

This result represents two intriguing points. One is that it is an unprecedented, highly precise measurement of m_W , and the other is that it is in about 7σ tension with the prediction of the standard model (SM), which is $m_W^{\text{SM}} = 80.379 \pm 0.006 \text{ GeV}$ [2]. Although the CDF result of m_W^{CDF} also shows a significant shift compared to the PDG average of the LEP [3], ATLAS [4] and the previous Tevatron [5] results yielding $m_W^{\text{PDG}} = 80.379 \pm 0.012 \text{ GeV}$ [6] as well as the result from LHCb leading to $m_W^{\text{LHCb}} = 80.354 \pm 0.031 \text{ GeV}$ [7], it may serve as a hint of new physics beyond the SM [8,9]. Under the assumption that the CDF measurement will be confirmed in the foreseeable future, it would deserve to explore its phenomenological implications.

The purpose of this work is to examine the implication of the recent measurement of the W boson mass at CDF II on

two-Higgs-doublet models (2HDMs). Recently, this possibility has been explored with different approaches in other works [10–15] and comprehensive analyses of the parameter space and other phenomenology have been performed not long ago (see, for example, Refs. [16–19]). The deviation of m_W^{CDF} from its SM prediction can be parametrized in terms of the so-called Peskin-Takeuchi parameters, S and T , which represent the contributions of new physics. The quantum corrections mediated by new scalar fields contribute to S and T . It is common belief that the exquisite precision achieved in the measurements of m_Z , m_W , and $\sin^2\theta_W$ makes it possible to explore the existence of new physics beyond the SM [20]. In this regards, another important parameter to test the SM is the so-called weak mixing angle parameter, $\sin^2\theta_W$ [20]. Instead of the on-shell definition of $\sin^2\theta_W$, it is more general to take it into account by employing the more theoretically motivated $\overline{\text{MS}}$ (modified minimal subtraction) prescription. All Z^0 pole measurements of $\sin^2\theta_W(m_Z)_{\overline{\text{MS}}}$ are usually averaged out to give

$$\sin^2\theta_W(m_Z)_{\overline{\text{MS}}}^{\text{ave}} = 0.23124 \pm 0.00006. \quad (2)$$

Equation (2) represents that the average of all Z^0 pole measurements is in consistent with the SM. But, the contributions of new physics to $\sin^2\theta_W(m_Z)_{\overline{\text{MS}}}$ can also be parametrized in terms of S and T parameters. Thus, the deviation of m_W from its SM prediction may, in general, affect the prediction of $\sin^2\theta_W(m_Z)_{\overline{\text{MS}}}$. In this work, we will first examine whether there exist nontrivial S and T parameters accommodating both m_W^{CDF} and

^{*} axionahn@naver.com

[†] skkang@seoultech.ac.kr

[‡] rayramosang@gmail.com

Published by the American Physical Society under the terms of the Creative Commons Attribution 4.0 International license. Further distribution of this work must maintain attribution to the author(s) and the published article's title, journal citation, and DOI. Funded by SCOAP³.

$\sin^2\theta_W(m_Z)_{\overline{\text{MS}}}^{\text{ave}}$, and compare them with those obtained from the global fit of Ref. [21]. Using the allowed regions of the parameter S and T from two observables m_W and $\sin^2\theta_W(m_Z)_{\overline{\text{MS}}}$, we will estimate the allowed regions of the masses of new scalar bosons and mixing angles in 2HDMs. To see the impact of the recent CDF W -boson mass on the parameter scan, we compare the results based on m_W^{CDF} with those based on m_W^{PDG} . In the analysis, we impose the theoretical conditions such as the vacuum stability, perturbativity [22,23] and unitarity [24,25], and experimental constraints to constrain the masses of Higgs fields and mixing parameters. Since the 125.1 GeV Higgs boson observed at the LHC can be either the lighter or heavier CP -even neutral scalar boson in the 2HDM, we divide our study in two scenarios, labeling as scenario 1 the case when the lighter Higgs mass, M_h , corresponds to the 125.1 GeV scalar; and scenario 2 to whenever the heavier Higgs takes that place. In addition, we study the phenomenological consequences of other observables that can be affected by m_W within the predictions of the 2HDM, most notably, the decay width of the Z boson. We expand on this idea by considering measurements of electroweak precision observables in the proposed Future Circular Lepton Collider (FCC-ee). The FCC-ee is the first step in the Future Circular Collider integrated program [26], and will consist of a 100 km underground circular machine that will take data over 15 years. Its implementation will follow an staged approach focusing on electroweak, flavor, Higgs, and top physics. For our analysis, we will focus on the electroweak precision observables prospects where the FCC-ee is expected to reduce the current uncertainties around 500 times [27] and see how they can distinguish both cases of m_W .

The rest of the paper is laid out as follows: In Sec. II, we give a brief summary of 2HDMs and present how the observables m_W and $\sin^2\theta_W$ can be parametrized in terms of S and T parameters. The allowed regions of S and T are obtained by imposing the recent CDF m_W and the PDG result of $\sin^2\theta(m_Z)_{\overline{\text{MS}}}$, and compare them with those obtained from the global fit of Ref. [21]. We also discuss on the various constraints from theoretical conditions and experimental results, which will be imposed in this analysis. In Sec. III, we show our numerical results and discuss the implications of CDF's measurement of m_W by incorporating the PDG result of $\sin^2\theta(m_Z)_{\overline{\text{MS}}}^{\text{ave}}$ in the scenarios mentioned above for 2HDM types I and II. Finally, in Sec. IV we discuss the most relevant details of this work and conclude.

II. TWO-HIGGS-DOUBLET MODEL

A. The setup

Taking Φ_1 and Φ_2 are two complex $SU(2)_L$ Higgs doublet fields with $Y = 1$, the renormalizable gauge invariant scalar potential of 2HDM with softly broken Z_2

symmetry under which $\Phi_1 \rightarrow \Phi_1$ and $\Phi_2 \rightarrow -\Phi_2$ is written as [28]

$$\begin{aligned}
 V = & m_{11}^2 \Phi_1^\dagger \Phi_1 + m_{22}^2 \Phi_2^\dagger \Phi_2 - (m_{12}^2 \Phi_1^\dagger \Phi_2 + \text{H.c.}) \\
 & + \frac{1}{2} \lambda_1 (\Phi_1^\dagger \Phi_1)^2 + \frac{1}{2} \lambda_2 (\Phi_2^\dagger \Phi_2)^2 \\
 & + \lambda_3 (\Phi_1^\dagger \Phi_1) (\Phi_2^\dagger \Phi_2) + \lambda_4 (\Phi_1^\dagger \Phi_2) (\Phi_2^\dagger \Phi_1) \\
 & + \left\{ \frac{1}{2} \lambda_5 (\Phi_1^\dagger \Phi_2)^2 + \text{H.c.} \right\}. \quad (3)
 \end{aligned}$$

We note that all the parameters in Eq. (3) to be real and the squared mass of pseudoscalar m_A^2 to be greater than $|\lambda_5|v^2$ so as to keep CP symmetry in the scalar potential.¹ As one can easily check, the dangerous flavor changing neutral currents is absent in the form given by Eq. (3) even if nonzero m_{12}^2 softly breaking the Z_2 symmetry is allowed.

Yukawa interactions of h and H are parametrized by

$$\mathcal{L}_{\text{yuk}} = - \sum_{f=u,d,l} \frac{m_f}{v} (\hat{y}_f^h \bar{f} f h + \hat{y}_f^H \bar{f} f H), \quad (4)$$

where the effective couplings of $\hat{y}_f^{h,H}$ are referred to [29]. Depending on how to couple the Higgs doublets to the fermions, 2HDMs are classified into four types [30]. Among them, the Yukawa couplings of 2HDM type II arises in the minimal supersymmetric standard model, which is one of the most promising candidates for the new physics model beyond the SM. In this work, we consider 2HDM type I and type II and present how the allowed regions of the masses of new scalars and mixing angles are different from each other.

The spontaneous breaking of electroweak symmetry triggers the generation of the vacuum expectation values of the Higgs fields as follows:

$$\langle \Phi_1 \rangle = \frac{1}{\sqrt{2}} \begin{pmatrix} 0 \\ v_1 \end{pmatrix}, \quad \langle \Phi_2 \rangle = \frac{1}{\sqrt{2}} \begin{pmatrix} 0 \\ v_2 \end{pmatrix}, \quad (5)$$

where $v^2 \equiv v_1^2 + v_2^2 = (246 \text{ GeV})^2$ with $v_2/v_1 = \tan\beta$, and v_1 and v_2 are taken positive, so that $0 \leq \beta \leq \pi/2$ is allowed. Then, the fluctuation fields around v_1 and v_2 become

$$\Phi_1 = \begin{pmatrix} \phi_1^+ \\ \frac{v_1 + \rho_1 + i\eta_1}{\sqrt{2}} \end{pmatrix}, \quad \Phi_2 = \begin{pmatrix} \phi_2^+ \\ \frac{v_2 + \rho_2 + i\eta_2}{\sqrt{2}} \end{pmatrix}. \quad (6)$$

Among the 8 degrees of freedom, three are eaten by the gauge bosons and the remaining five become physical Higgs particles in 2HDM: two CP -even neutral Higgses h

¹The other terms generally allowed in the scalar potential are ignored to keep CP symmetry.

and H ($M_h \leq M_H$), a CP -odd neutral Higgs A and a charged Higgs pair (H^\pm). The neutral scalars are given by

$$\begin{aligned} h &= \sqrt{2}(\eta_2 \sin \alpha - \eta_1 \cos \beta), \\ H &= -\sqrt{2}(\eta_2 \cos \alpha + \eta_1 \sin \beta), \\ A &= \sqrt{2}(\rho_2 \sin \beta - \rho_1 \cos \beta). \end{aligned} \quad (7)$$

Following Ref. [28], the squared masses for the CP -odd and charged Higgs states are calculated to be

$$M_A^2 = \frac{m_{12}^2}{s_\beta c_\beta} - \lambda_5 v^2, \quad M_{H^\pm}^2 = M_A^2 + \frac{1}{2}v^2(\lambda_5 - \lambda_4), \quad (8)$$

and the squared masses for neutral Higgs ($M_H \geq M_h$) are given by [28]

$$M_{H,h}^2 = \frac{1}{2}[P + Q \pm \sqrt{(P - Q)^2 + 4R^2}], \quad (9)$$

where $P = \lambda_1 v_1^2 + m_{12}^2 t_\beta$, $Q = \lambda_2 v_2^2 + m_{12}^2 / t_\beta$, and $R = (\lambda_3 + \lambda_4 + \lambda_5)v_1 v_2 - m_{12}^2$ with $s_\beta = \sin \beta$, $c_\beta = \cos \beta$, and $t_\beta = \tan \beta$. While h becomes the SM-like Higgs boson for $\sin(\beta - \alpha) = 1$, H does so for $\cos(\beta - \alpha) = 1$. In this work, we examine the implications of the recent CDF W -boson mass in both cases separately.

B. W -boson mass and $\sin^2 \theta_W(m_Z)_{\overline{\text{MS}}}$

The contribution of new scalar fields to T and S parameters are given by [31–34]

$$\begin{aligned} T &= \frac{\sqrt{2}G_F}{16\pi^2 \alpha_{\text{EM}}} \{ -F'(M_A, M_H^\pm) \\ &\quad + \sin^2(\beta - \alpha)[F'(M_H, M_A) - F'(M_H, M_{H^\pm})] \\ &\quad + \cos^2(\beta - \alpha)[F'(M_h, M_A) - F'(M_h, M_{H^\pm})] \}, \end{aligned} \quad (10)$$

$$\begin{aligned} S &= -\frac{1}{4\pi} [F(M_{H^\pm}, M_{H^\pm}) - \sin^2(\beta - \alpha)F(M_H, M_A) \\ &\quad - \cos^2(\beta - \alpha)F(M_h, M_A)], \end{aligned} \quad (11)$$

where the functions F and F' are given by [31–33,35–37]

$$\begin{aligned} F(x, y) &= -\frac{1}{3} \left[\frac{4}{3} - \frac{x^2 \ln x^2 - y^2 \ln y^2}{x^2 - y^2} \right. \\ &\quad \left. - \frac{x^2 + y^2}{(x^2 - y^2)^2} \left(1 + \frac{x^2 + y^2}{2} - \frac{x^2 y^2}{x^2 - y^2} \ln \frac{x^2}{y^2} \right) \right], \end{aligned} \quad (12)$$

$$F'(x, y) = \frac{x^2 + y^2}{2} - \frac{x^2 y^2}{x^2 - y^2} \ln \frac{x^2}{y^2}. \quad (13)$$

Employing the precise measurements of QED coupling α , G_F , and m_Z accompanied by m_t and $M_{h_{\text{SM}}} = 125.1$ GeV,

and allowing for loop effects mediated by heavy new particles via S and T parameters, we can recast the expressions for the predictions of m_W and $\sin^2 \theta_W(m_Z)_{\overline{\text{MS}}}$ as follows [20]

$$m_W = 80.357 \text{ GeV}(1 - 0.0036S + 0.0056T), \quad (14)$$

$$\sin^2 \theta_W(m_Z)_{\overline{\text{MS}}} = 0.23124(1 + 0.0157S - 0.0112T). \quad (15)$$

Plugging the experimental values for m_W , from Eq. (1), and $\sin^2 \theta_W(m_Z)_{\overline{\text{MS}}}$, from Eq. (2), into Eqs. (14) and (15) we obtain the allowed regions of S and T parameters as follows:

$$\begin{aligned} T &= 0.3 \pm 0.062, \\ S &= 0.2 \pm 0.08. \end{aligned} \quad (16)$$

Those results may indicate that the contributions of new physics are prominent in m_W while they are canceled in $\sin^2 \theta_W(m_Z)_{\overline{\text{MS}}}$. Note that these values are in agreement with the values obtained in Ref. [21]. To be precise, the value of S is shifted $\sim 25\%$ in our work with the same error of roughly 50%. In the case of T the shift is only $\sim 10\%$ and the errors (roughly 20%) are almost identical. In our numerical analysis, we study how the masses of new scalar fields and mixing angles in 2HDM can be constrained by imposing the results of Eq. (16). Thus, our results are more affected by the CDF m_W value than from directly using the values from the global fit.

C. The bounds

The vacuum stability of the scalar potential, Eq. (3), is guaranteed only if the following conditions are satisfied [23,28]

$$\lambda_{1,2} > 0, \quad \lambda_3 > -\sqrt{\lambda_1 \lambda_2}, \quad \lambda_3 + \lambda_4 - |\lambda_5| > -\sqrt{\lambda_1 \lambda_2}. \quad (17)$$

The stability conditions of Eq. (17) give rise to lower bounds on the couplings λ_i [28], which in turn lead to bounds on the masses of the physical Higgs fields. In addition, we require that the quartic couplings λ_i in the scalar potential is perturbative and unitarity conditions [24] are satisfied. Those theoretical conditions can constrain not only the masses of the Higgs fields but also mixing parameters $\tan \beta$ and α .

On the other hand, we can consider the experimental constraints. Since the Higgs-strahlung at the LEP is one of the most direct channels to probe a light Higgs boson h with mass below 120 GeV, we use the strongest upper bound on the event rate of $e^+e^- \rightarrow Zh \rightarrow Zjj$ [38,39] to constrain the mass and mixing parameters. We also consider the constraints coming from the Higgs pair production process, $e^+e^- \rightarrow hA \rightarrow b\bar{b}b\bar{b}$ when the mass parameters are kinematically allowed [39]. The experimental lower bound on charged Higgs masses is 79.3 GeV [40]. The

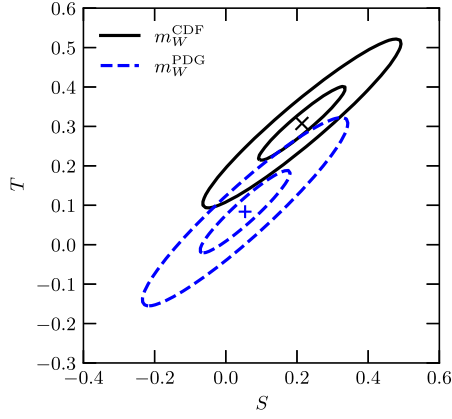


FIG. 1. Contours for the S and T oblique parameters obtained with Eqs. (14) and (15). The black solid contours correspond to the value obtained using the value recently announced by the CDF Collaboration, the blue dashed contours is obtained using the previous average 80.379 ± 0.012 GeV. The interior (exterior) contour corresponds to 1σ (3σ).

nonobservation of $Z \rightarrow hA$ in the LEP experiment gives rise to the condition that $M_h + M_A > M_Z$ are kinematically allowed [41]. We include the upper bounds on $\text{Br}(t \rightarrow H^+ b) \times \text{Br}(H^+ \rightarrow \tau^+ \nu_\tau)$ coming from the LHC search for H^\pm through the channel $pp \rightarrow t\bar{t} \rightarrow b\bar{b}H^\pm W^\mp$ followed by $H^\pm \rightarrow \tau^\pm \nu$ [42–44]. The results from the LHC Higgs signal strengths at 7 and 8 TeV are taken into account.

In addition to the above constraints explained, we take into account the measurement of $R_b \equiv \Gamma(Z \rightarrow b\bar{b})/\Gamma(Z \rightarrow \text{hadrons})$ [6]. The updated SM prediction of $B_{\text{SM}}(\bar{B} \rightarrow X_s \gamma)$ [45] and the Belle experiment [46] give a severe bound on M_{H^\pm} in the type II; with the lower bound at 95% C.L. for M_{H^\pm} in the range 570–800 GeV [47]. The measurements of $B - \bar{B}$ mixing also lead to the constraints on the $M_{H^\pm} - \tan\beta$ plane but less severe ones in comparison with that from R_b [48]. Combining the theoretical constraints with the experimental ones as done in Refs. [29,49], we can investigate how the masses of Higgs bosons and mixing parameters can be constrained.

III. RESULTS AND DISCUSSION

In this section we present the analysis performed and discuss relevant details of the results. The contribution from the oblique parameter U is expected to be negligible compared to the contributions from S and T . Using Eqs. (15) we obtain the limits cited in Eq. (16). The two-dimensional contours are shown in Fig. 1 including the value obtained using the previous average that is consistent with the SM. In what follows we describe the rest of the components of our numerical analysis.

A. Methodology

We begin by enforcing the conditions of unitarity, perturbativity, and stability of the potential, by requiring

that Eqs. (17) are respected. These theoretical conditions are applied as hard cuts to ensure that every sampled point is theoretically meaningful. Considering that the oblique parameters, dominantly S and T , shift the value for $\sin^2\theta_W(m_Z)_{\overline{\text{MS}}}$, we will require their values to be consistent with both the recent measurement of the mass of the W^\pm by the CDF collaboration and with the current experimental average for the weak mixing angle. To calculate the theoretical constraints and oblique parameters, as well as other observables we employ 2HDMC [25]. This tool is then interfaced with HiggsBounds [50] and HiggsSignals [51] to incorporate several constraints from LEP, Tevatron, and LHC on the Higgs sector and obtain a χ^2 for the currently observed signals of the Higgs. Finally, to calculate flavor physics observables, that will be relevant mostly for the 2HDM-II as mentioned in Sec. II C, we process our obtained data with SUPERISO [52]. We use the Markov Chain Monte Carlo sampler EMCEE [53] to explore the parameter space. The free parameters of our model are given by the mass of the heavy Higgs, m_H , the charged Higgs mass, m_{H^\pm} , the mass of the pseudoscalar, m_A , the mixing $\cos(\beta - \alpha)$, the parameter $\tan\beta$ and the squared mass parameter m_{12}^2 . The limits of our parameter scan are given by

$$\begin{aligned}
 M_H/1 \text{ TeV}: & \text{ type I: } [0.13, 1], \text{ type II: } [0.13, 1.9], \\
 M_{H^\pm}/1 \text{ TeV}: & \text{ type I: } [0.08, 1], \text{ type II: } [0.15, 1.9], \\
 M_A/1 \text{ TeV}: & \text{ type I: } [0.02, 1], \text{ type II: } [0.02, 1.9], \\
 \cos(\beta - \alpha): & [-0.5, 0.5], \\
 \tan\beta: & [0.1, 20], \\
 m_{12}^2/1 \text{ GeV}^2: & [0, 500^2],
 \end{aligned} \tag{18}$$

where the larger upper bound for type II considers the higher lower bound on M_{H^\pm} imposed by flavor physics as mentioned in Sec. II C.

The recent measurement of the mass of the W^\pm that we use to constrain our parameter space is given in Eq. (1). We will also use the average published by the PDG collaboration, given by $m_W^{\text{PDG}} = 80.379 \pm 0.012$, to compare the parameter space that leads to these two different measurements. We fix the mass of the lighter CP -even Higgs to the current average central value of the SM Higgs $m_h = 125.10$ GeV [6].

B. Scenario 1: 2HDM-I

It is well known that the parameters S and T give the largest contribution to the shift in m_W . From Eqs. (10) and (11) we can see that in the 2HDM they are largely affected by mass differences between scalars. Expectedly, we find that to predict the mass of the W^\pm boson in the range measured by the CDF Collaboration we require sizable mass splittings. Different mass splittings and their resulting

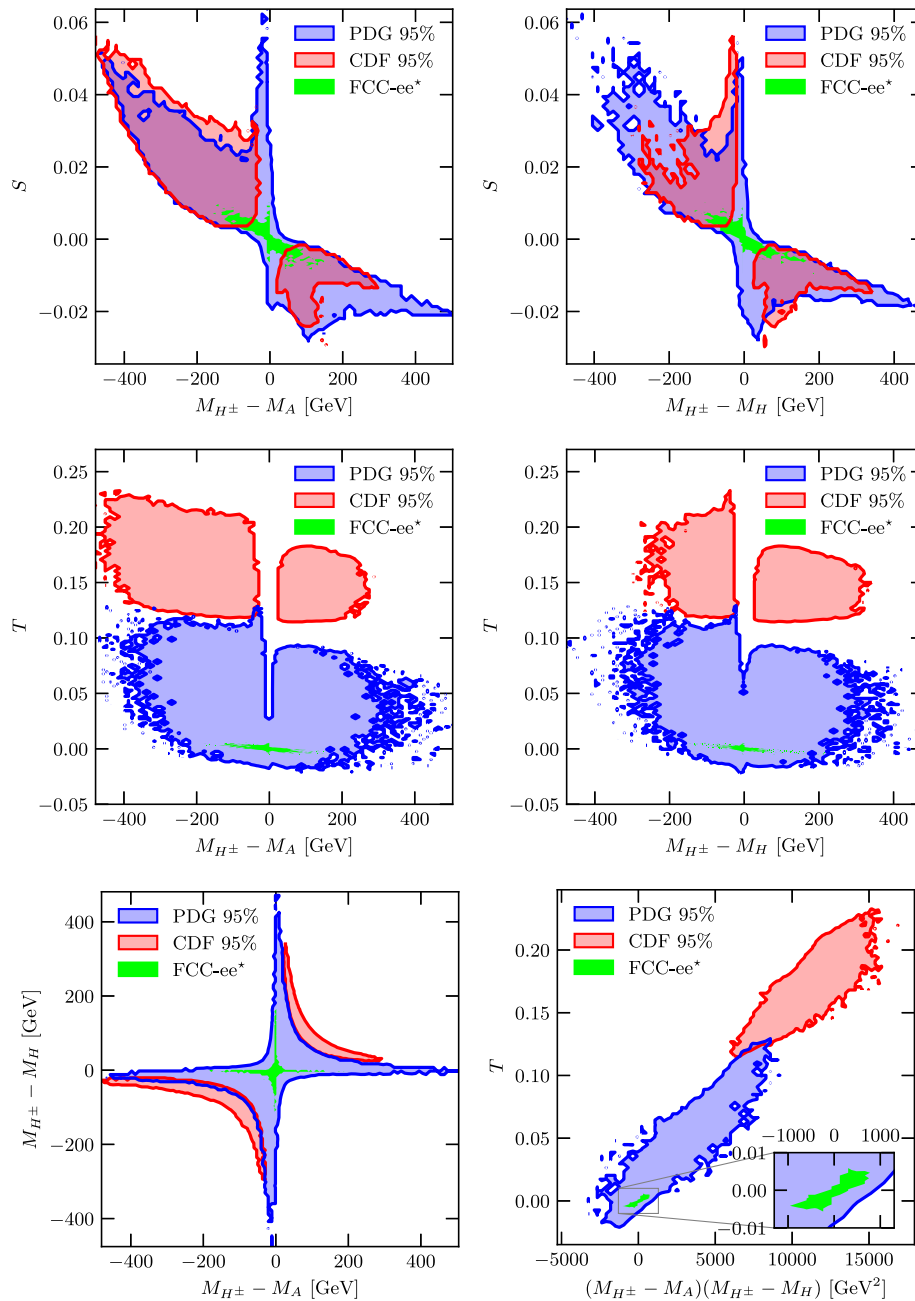


FIG. 2. Scenario 1, type I: Dependence of S (upper) and T (medium) parameters on the mass splittings ($M_{H^\pm} - M_A$) (upper and medium-left) and ($M_{H^\pm} - M_H$) (upper and medium-right). On the bottom, relation between mass splittings (left) and the dependence of T on the product of these splittings (right). Regions consistent with CDF-II measurement of m_W are shown in red, while regions in blue correspond to the average published by the PDG. The green region corresponds to the estimated sensitivity for FCC-ee [27] around the SM prediction (*see text for details).

values for S and T are shown in Fig. 2. When comparing the contours at 95% C.L. for the PDG average (blue) and the CDF measurement (red) we see that the CDF measurement requires a higher value for T . We also depict a green region for the projected sensitivity of FCC-ee [27] at 95% C.L. that will be explained in detail later. In the case of the CDF measurement, for S and T we observe that both splittings $M_{H^\pm} - M_A$ and $M_{H^\pm} - M_H$ are required to be

simultaneously and always nonzero. Closer inspection of Eqs. (10) and (11) shows that if both splittings vanish simultaneously then S and T would vanish as well. This case results in m_W as predicted by the SM and is well inside the region using the PDG average value. From the separation of the contours in the figures with T axis, we can infer that T has the largest contribution to the shift in the mass of the W^\pm . In the bottom panels of Fig. 2 we can

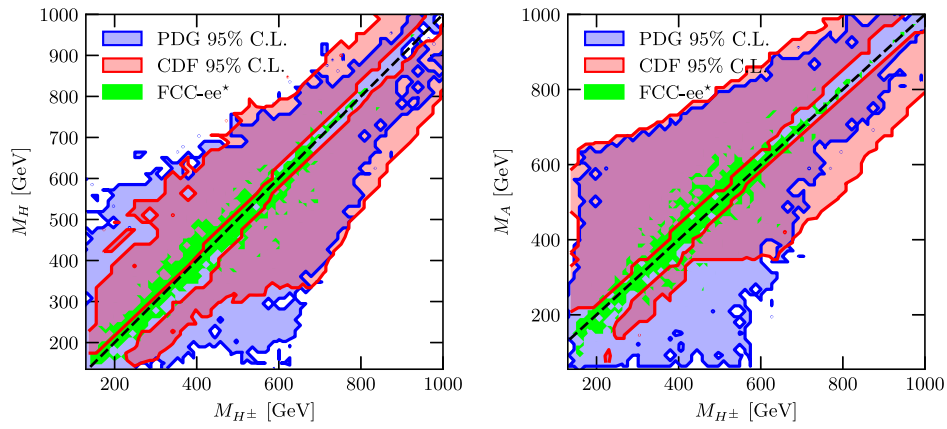


FIG. 3. Scenario 1, type I: Dependence of the scalars and pseudoscalar masses on each other. The colors are as in Fig. 2. The diagonal $x = y$ is represented by the dashed black line.

see the relation between the two mass differences, $M_{H^\pm} - M_A$ and $M_{H^\pm} - M_H$ (bottom left), and that the allowed regions of their combination are almost separated for both cases of m_W (bottom right). In particular, we see that the regions follow hyperboliclike contours that tend to be in regions where both mass differences have the same sign, with the CDF measurement in regions with simultaneous larger mass differences. This hyperbolic behavior hints to an effective dependence of T on the product of mass differences, which is demonstrated in the bottom-right panel of Fig. 2.

Since the size of the parameters S and T depends heavily on the splittings between scalars and pseudoscalar we can expect their mass ranges to depend notably on the masses of each other. This is illustrated in Fig. 3, where the first notable feature is how the diagonal for equal masses splits the CDF region in two, something that does not happen for the PDG average. This is because of the need of nonzero mass differences as shown in Fig. 2. The relationship

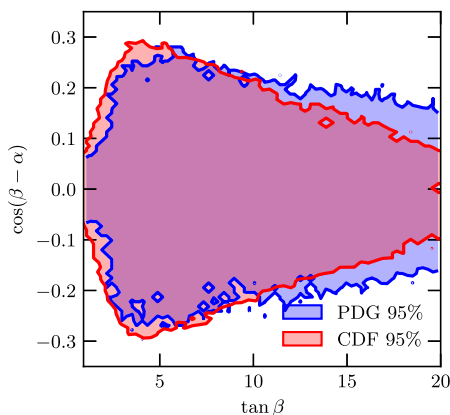


FIG. 4. Scenario 1, type I: Relationship between $\tan\beta$ and $\cos(\beta - \alpha)$. The colors are as in Fig. 2 except for FCC-ee contour which has almost no effect for this combination of parameters. There is some reduction in $\cos(\beta - \alpha)$ range for large $\tan\beta$ due to data thinning that does not affect other results.

between $\tan\beta$ and $\cos(\beta - \alpha)$, the latter being the mixing between Higgses, is shown in Fig. 4. In this case we can see that the range of $\cos(\beta - \alpha)$ is not obviously affected by the change in W^\pm mass.

Up to this point, it is clear that the biggest difference between CDF and PDG regions appears when projecting on the T parameter. The size of the T parameter strongly affects the prediction for the decay width of the Z [54,55] (see also Sec. 10 of Ref. [6]), which is explicitly demonstrated in Fig. 5. Besides the decay width of the Z boson, both parameters, S and T , can have effects on other electroweak precision observables. With this in mind, we estimate the future allowed region using the projected error bars from the proposed Future Circular Lepton Collider (FCC-ee) as reported in Table 3 of Ref. [27]. In particular, we use projected sensitivities for measurements of Z properties: decay width (Γ_Z), the ratios of hadrons to

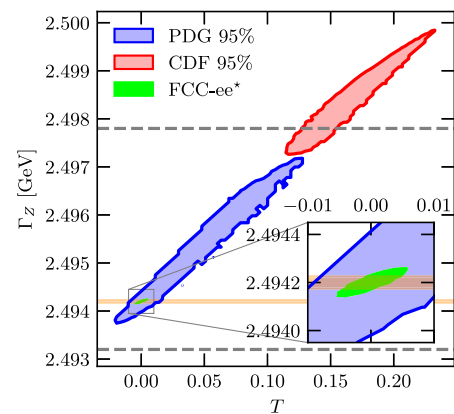


FIG. 5. Scenario 1, type I: Predicted decay width of the Z boson, Γ_Z , for the allowed CDF and PDG regions. The dashed lines and orange band mark the 1σ range for Γ_Z using the current average [6] and the FCC-ee projected sensitivity, respectively. The green region corresponds to the estimated sensitivity for FCC-ee around the SM prediction for several observables (* see text for details).

leptons partial decay widths (R_ℓ^Z), the ratio of $b\bar{b}$ to hadrons partial decay widths (R_b), and the hadronic cross section (σ_{had}), as well as the projected error bar on the mass of the W . We add statistical and systematic errors in quadrature and assume that the central value will be consistent with the SM. The resulting constraints on the allowed region is quite severe as is clearly seen in the 95% C.L. green regions in Figs. 2 and 3. In Fig. 2 we can see that the sizes for S and T are reduced down to $\mathcal{O}(10^{-2})$ or less. The effect on the mass splittings is more clear when we consider the

combination of them, as can be seen in the bottom panels of the same figure. We can see that for FCC-ee, at least one of the two mass differences displayed has to be close to zero resulting in a very small allowed region for their product. This is reflected in Fig. 3, where we can find the FCC-ee consistent regions mostly around the dashed diagonal line. Considering the results of this analysis, if the 2HDM-I is responsible for the deviation in the mass of the W , the FCC-ee should see further deviations in other observables, most notably Γ_Z . So, we can expect that the

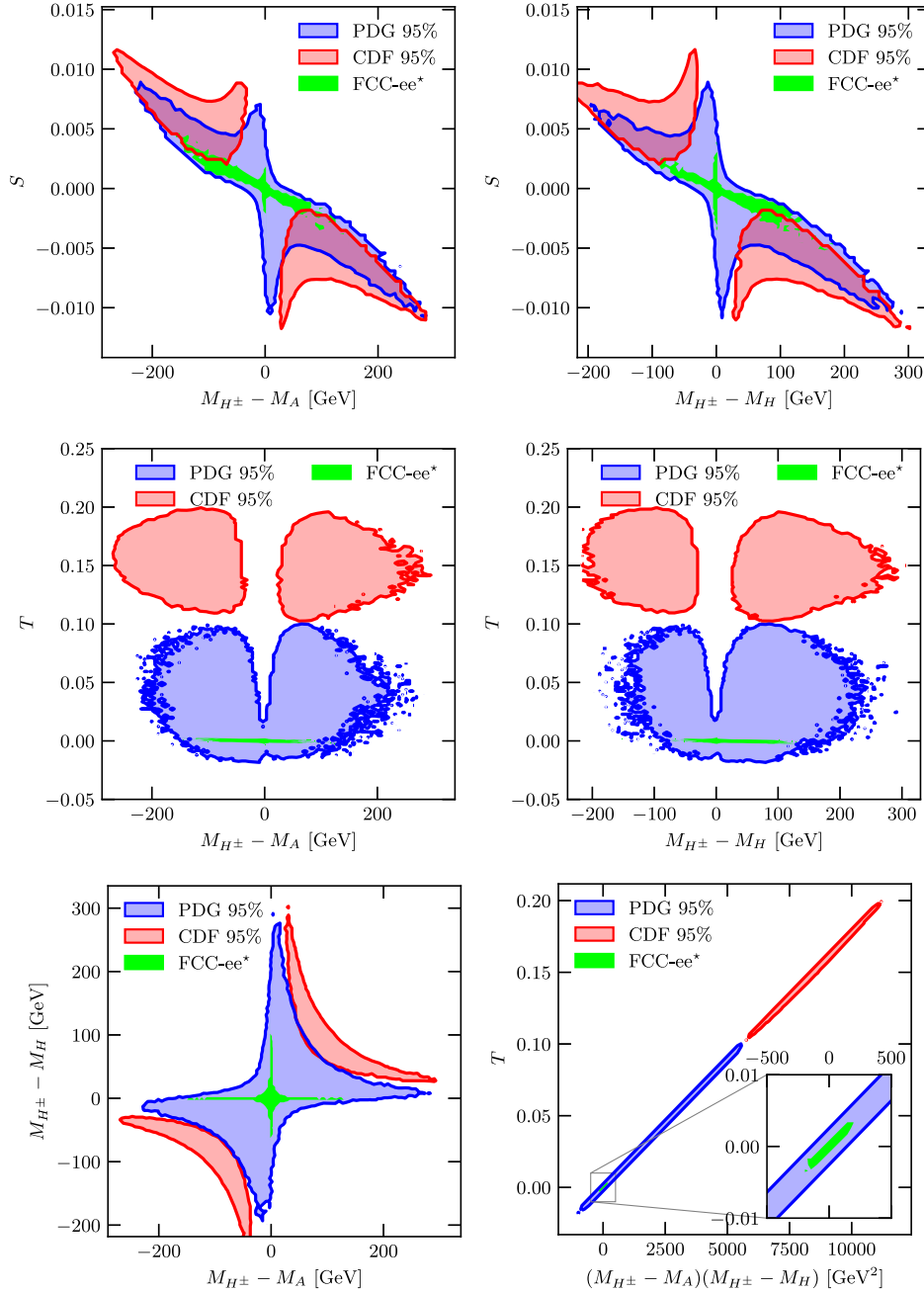


FIG. 6. Scenario 1, type II: dependence of S (upper) and T (medium) parameters on the mass splittings ($M_{H^\pm} - M_A$) (upper and medium left) and ($M_{H^\pm} - M_H$) (upper and medium right). On the bottom, relation between mass splittings (left) and the dependence of T on the product of these splittings (right). The colors are as in Fig. 2.

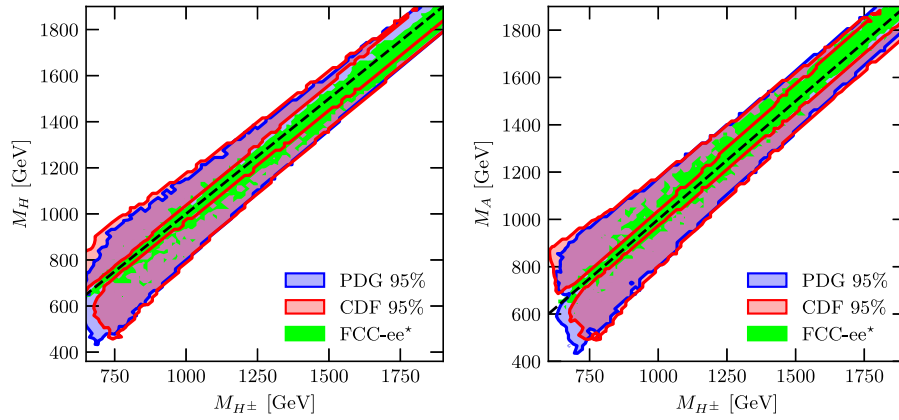


FIG. 7. Scenario 1, type II: dependence of the scalars and pseudoscalar masses on each other. The colors are as in Fig. 2. The diagonal $x = y$ is represented by the dashed black line.

FCC-ee would decisively support or rule out the CDF measurement. To finalize this part, the FCC-ee improvement is not expected to have an important effect on $\tan\beta$ or $\cos(\beta - \alpha)$ and is, therefore, not shown in Fig. 4.

C. Scenario 1: 2HDM-II

In the case of the 2HDM-II we see some of the same features such as the need for nonzero mass differences for H^\pm , A , and H . As before, in Fig. 6 we see a clear separation between the values of T that are required for the W^\pm mass measured by CDF and the PDG average. However, we see that in this case the range of the difference $M_{H^\pm} - M_A$ is slightly smaller than it was for 2HDM-I. For S , we find values much smaller ranging approximately between $[-0.01, 0.01]$ and we see less overlap between both regions. In the bottom panels of Fig. 6, we see again that the mass differences have a hyperbolic behavior, as in the case of 2HDM-I, although with smaller ranges. This results in a very narrow relationship between the product of mass differences and T , as can be seen on the bottom right panel.

The most notable feature of 2HDM-II is the effects of the charged Higgs, H^\pm , in flavor physics observables, most importantly in $\bar{B} \rightarrow X_s \gamma$, resulting in a lower bound for M_{H^\pm} . In Fig. 7 we see the allowed regions projected in the planes $M_{H^\pm} - M_H$ (left) and $M_{H^\pm} - M_A$ (right). Again, we see that the equal masses diagonal splits the CDF regions in two sections. In the same figure, both panes display a lower bound for M_{H^\pm} that is taken to be around 650 GeV, well inside the expected range for the 95% C.L. lower bound found in Ref. [47], although the precise value could change with a proper, dedicated study on the observables affected by the H^\pm . Such study is out of the scope of this work.

We show the relationship between $\tan\beta$ and $\cos(\beta - \alpha)$ in Fig. 8. Similar to type I, there is no considerable change in the allowed contours from using the two different results for m_W . However, we note that in this case the resulting

range for $\cos(\beta - \alpha)$ is approximately 10 times smaller that it was for type I, reflecting that the decoupling limit $\sin(\beta - \alpha) \sim 1$ is preferred.

In this case we also apply the same analysis as in the previous part, using the projected sensitivity by FCC-ee. Expectedly, the results are very similar to the ones described for 2HDM-I above, with S and T reduced to $\mathcal{O}(10^{-2})$ sizes or less and at least one mass difference forced to be much closer to zero than the other. Due to the narrower ranges for the mass differences, that also result in a much narrower S , the predicted regions at 95% C.L. for the decay width of the Z in Fig. 9 are much thinner than in the case of the 2HDM-I as can be seen in Fig. 5. However, the same conclusion can be drawn about FCC-ee being able to observe deviations in other observables, such as Γ_Z . Again, the FCC-ee projected sensitivity does not significantly affect $\tan\beta$ and $\cos(\beta - \alpha)$ and we do not show its region in Fig. 8.

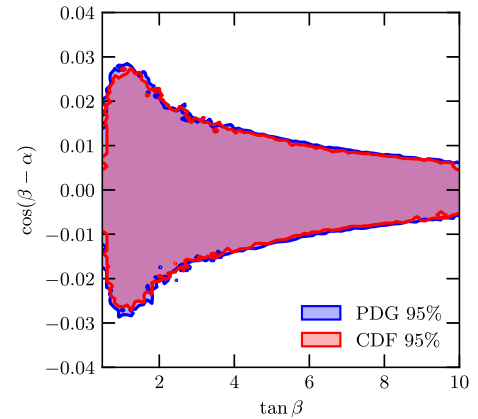


FIG. 8. Scenario 1, type II: relationship between $\tan\beta$ and $\cos(\beta - \alpha)$. The colors are as in Fig. 2 except for the FCC-ee contour, which has almost no effect for this combination of parameters.

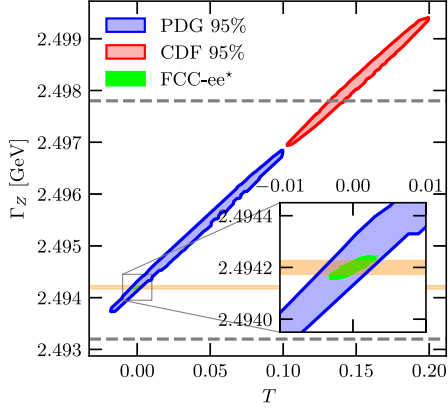


FIG. 9. Predicted decay width of the Z boson, Γ_Z , for the allowed CDF and PDG regions. The dashed lines and orange band mark the 1σ range for Γ_Z using the current average [6] and the FCC-ee projected sensitivity, respectively. The green region uses the estimated sensitivity for FCC-ee around the SM prediction for several observables (*see text for details).

D. Scenario 2: 2HDM-I

Scenario 2, where the mass of the lighter CP -even neutral scalar is chosen as $M_h < 125.1$ GeV, presents

several complications due to the loss of freedom compared to scenario 1. First of all, considering that the mass differences required to predict the CDF measured m_W belong in the ranges of $\mathcal{O}(10)$ GeV to a few $\mathcal{O}(190)$ GeV we can expect the mass difference $M_{H^\pm} - M_h$ predominantly positive. From what we saw in the results of previous cases we can say that this will limit the values of S to be mostly negative. This will heavily affect our allowed ranges, since, from Eq. (16), we know that S is preferred positive. In fact, from our analysis, we find that this scenario results in a value for $\sin^2\theta_W(m_Z)_{\overline{\text{MS}}}$ that is just marginally inside its 3σ region. This is confirmed in Fig. 10, where we can see in the upper two panes that CDF measurement of m_W prefers S below -0.02 . Note that in Fig. 10 the tension with the measured $\sin^2\theta_W(m_Z)_{\overline{\text{MS}}}$ has been ignored for the red contour to display the region that predicts m_W^{CDF} . Also, we see that the preferred range for $M_{H^\pm} - M_h$ is almost entirely positive and reaches up to ~ 600 GeV. In the case of T , this results in one connected region corresponding to positive mass differences in contrast to the scenario 1 where T had two disconnected regions for positive and negative mass differences. From scenario 1 we learned that the preferred values of S and T

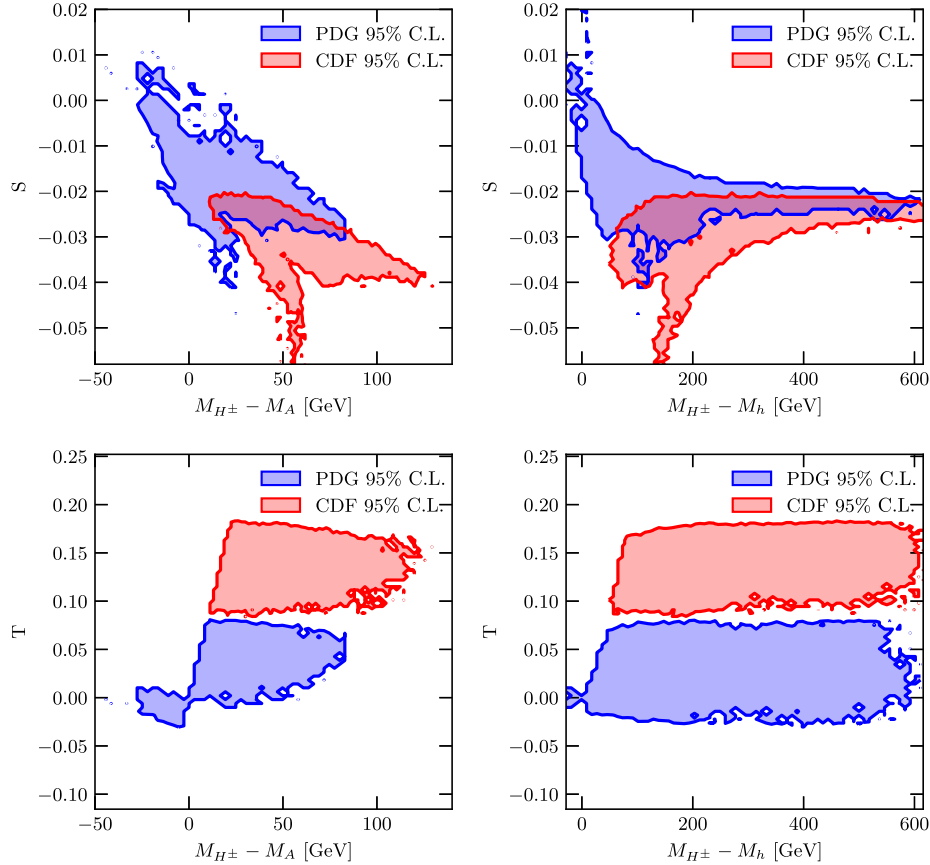


FIG. 10. Scenario 2, type I: dependence of the S (upper) and T (lower) parameters on the mass splittings between $H^\pm - A$ (left) and $H^\pm - H$ (right). For the red contour, tension with measured $\sin^2\theta_W(m_Z)_{\overline{\text{MS}}}$ has been ignored to show the regions that reproduces the CDF measurement of m_W .

happened simultaneously for $M_{H^\pm} - M_A$ and $M_{H^\pm} - M_{A'}$ negative, therefore, we can conclude that 2HDM-I in scenario 2 is disfavored by requiring a light CP -even neutral state. Considering this result, in this scenario we do not apply the analysis on future prospects for FCC-ee.

E. Scenario 2: Brief comment on 2HDM-II

From Sec. III D we learned that requiring a CP -even neutral state lighter than 125.1 GeV resulted in less freedom and more constrained parameter space. In particular, having the correct size for $M_{H^\pm} - M_h$ in this case results in a lighter M_{H^\pm} since the required mass differences are of a few 100 GeV at most. This is particularly problematic in 2HDM-II, where $\bar{B} \rightarrow X_s \gamma$ strongly constrains light M_{H^\pm} . We find that the mass M_{H^\pm} required to predict m_W^{CDF} is light enough to be in tension with flavor physics measurements, since, as can be seen in Fig. 7, the charged Higgs is constrained to be above ~ 600 GeV.

IV. CONCLUSION

In this work we attempted to constrain the 2HDM parameter space based on the new measurement of a 7σ deviation from the SM for the mass of the W^\pm boson, m_W . Interestingly, we found that by combining the relationship of m_W and $\sin^2(m_Z)_{\text{MS}}$ with the S and T parameters we can constrain those parameters at a level consistent with more

complete global fits [21]. We demonstrated that using this constraint, together with the usual theoretical conditions and several observations from LEP, Tevatron, and LHC, there is a set of parameters that is compatible with the new measurement and, therefore, the 2HDM could successfully survive if the deviation on m_W is confirmed in the future. In particular, we found that the scenario where the Higgs found at the LHC having 125.1 GeV is identified as the light CP -even neutral scalar is more favored compared to the scenario where it corresponds to the heavier state. We show how important the mass splittings are to shift the W^\pm mass from its value predicted in the SM, mostly via the contribution from the oblique parameter T . We found clear differences between the requirements of the parameter space depending on the predicted W^\pm mass. Most notably, the required value of T takes nonoverlapping regions when one considers the two options of the CDF measurement and the PDG average. On the side of future prospects, we showed how an improved measurement of Z pole observables at the FCC-ee should clearly distinguish 2HDM hints on deviations to the SM. In our case, we found that if the 2HDM explains the newly measured m_W^{CDF} FCC-ee should observe a clear deviation from the SM expectation, particularly for the decay width of the Z . Indeed, future experimental observations may bring more exciting clues about where to focus theoretical efforts.

-
- [1] T. Aaltonen *et al.* (CDF Collaboration), High-precision measurement of the W boson mass with the CDF II detector, *Science* **376**, 170 (2022).
- [2] M. Awramik, M. Czakon, A. Freitas, and G. Weiglein, Precise prediction for the W boson mass in the standard model, *Phys. Rev. D* **69**, 053006 (2004).
- [3] S. Schael *et al.* (ALEPH, DELPHI, L3, OPAL, and LEP Electroweak Collaborations), Electroweak measurements in electron-positron collisions at W -boson-pair energies at LEP, *Phys. Rep.* **532**, 119 (2013).
- [4] M. Aaboud *et al.* (ATLAS Collaboration), Measurement of the W -boson mass in pp collisions at $\sqrt{s} = 7$ TeV with the ATLAS detector, *Eur. Phys. J. C* **78**, 110 (2018); Erratum, *Eur. Phys. J. C* **78**, 898 (2018).
- [5] T. A. Aaltonen *et al.* (CDF and D0 Collaborations), Combination of CDF and D0 W -boson mass measurements, *Phys. Rev. D* **88**, 052018 (2013).
- [6] P. A. Zyla *et al.* (Particle Data Group), Review of Particle Physics, *Prog. Theor. Exp. Phys.* **2020**, 083C01 (2020).
- [7] R. Aaij *et al.* (LHCb Collaboration), Measurement of the W boson mass, *J. High Energy Phys.* **01** (2022) 036.
- [8] For a study concerned with a possible hint of new physics coming from m_W measured at LEP, see, K. Kang and S. K. Kang, The minimal supersymmetric standard model and precision of W boson mass and top quark mass, *Mod. Phys. Lett. A* **13**, 2613 (1998).
- [9] D. Borah, S. Mahapatra, and N. Sahu, Singlet-doublet fermion origin of dark matter, neutrino mass and W -mass anomaly, [arXiv:2204.09671](https://arxiv.org/abs/2204.09671); J. Cao, L. Meng, L. Shang, S. Wang, and B. Yang, Interpreting the W mass anomaly in the vectorlike quark models, [arXiv:2204.09477](https://arxiv.org/abs/2204.09477); S. Baek, Implications of CDF W -mass and $(g-2)_\mu$ on $U(1)_{L_\mu-L_\tau}$ model, [arXiv:2204.09585](https://arxiv.org/abs/2204.09585); A. Bhaskar, A. A. Madathil, T. Mandal, and S. Mitra, Combined explanation of W -mass, muon $g-2$, $R_{K^{(*)}}$ and $R_{D^{(*)}}$ anomalies in a singlet-triplet scalar leptoquark model, [arXiv:2204.09031](https://arxiv.org/abs/2204.09031); K. Ghorbani and P. Ghorbani, W -boson mass anomaly from scale invariant 2HDM, [arXiv:2204.09001](https://arxiv.org/abs/2204.09001); M. Du, Z. Liu, and P. Nath, CDF W mass anomaly in a Stueckelberg extended standard model, [arXiv:2204.09024](https://arxiv.org/abs/2204.09024); Y. P. Zeng, C. Cai, Y. H. Su, and H. H. Zhang, Extra boson mix with Z boson explaining the mass of W boson, [arXiv:2204.09487](https://arxiv.org/abs/2204.09487); D. Borah, S. Mahapatra, D. Nanda, and N. Sahu, Type II Dirac Seesaw with observable ΔN_{eff} in the light of W -mass anomaly, [arXiv:2204.08266](https://arxiv.org/abs/2204.08266); O. Popov and R. Srivastava, The triplet Dirac Seesaw in the view of the recent CDF-II W mass anomaly, [arXiv:2204.08568](https://arxiv.org/abs/2204.08568); L. M. Carpenter, T. Murphy, and M. J. Smylie, Changing patterns in electroweak

- precision with new color-charged states: Oblique corrections and the W boson mass, [arXiv:2204.08546](#); K. Y. Zhang and W. Z. Feng, Explaining W boson mass anomaly and dark matter with a $U(1)$ dark sector, [arXiv:2204.08067](#); K. I. Nagao, T. Nomura, and H. Okada, A model explaining the new CDF II W boson mass linking to muon $g-2$ and dark matter, [arXiv:2204.07411](#); S. Kanemura and K. Yagyu, Implication of the W boson mass anomaly at CDF II in the Higgs triplet model with a mass difference, [arXiv:2204.07511](#); J. Kawamura, S. Okawa, and Y. Omura, W boson mass and muon $g-2$ in a lepton portal dark matter model, [arXiv:2204.07022](#); A. Crivellin, M. Kirk, T. Kitahara, and F. Mescia, Correlating $t \rightarrow cZ$ to the W mass and B physics with vector-like quarks, [arXiv:2204.05962](#); M. Endo and S. Mishima, New physics interpretation of W -boson mass anomaly, [arXiv:2204.05965](#); X. K. Du, Z. Li, F. Wang, and Y. K. Zhang, Explaining the new CDFII W -boson mass in the Georgi-Machacek extension models, [arXiv:2204.05760](#); K. Cheung, W. Y. Keung, and P. Y. Tseng, Iso-doublet vector leptoquark solution to the muon $g-2$, R_{K,K^*} , R_{D,D^*} , and W -mass anomalies, [arXiv:2204.05942](#); R. Balkin, E. Madge, T. Menzo, G. Perez, Y. Soreq, and J. Zupan, On the implications of positive W mass shift, [arXiv:2204.05992](#); T. Biekötter, S. Heinemeyer, and G. Weiglein, Excesses in the low-mass Higgs-boson search and the W -boson mass measurement, [arXiv:2204.05975](#); N. V. Krasnikov, Nonlocal generalization of the SM as an explanation of recent CDF result, [arXiv:2204.06327](#); A. Paul and M. Valli, Violation of custodial symmetry from W -boson mass measurements, [arXiv:2204.05267](#); L. Di Luzio, R. Gröber, and P. Paradisi, Higgs physics confronts the M_W anomaly, [arXiv:2204.05284](#); E. Bagnaschi, J. Ellis, M. Madigan, K. Mimasu, V. Sanz, and T. You, SMEFT analysis of m_W , [arXiv:2204.05260](#); J. J. Heckman, Extra W -boson mass from a D3-brane, [arXiv:2204.05302](#); H. M. Lee and K. Yamashita, A model of vector-like leptons for the muon $g-2$ and the W boson mass, [arXiv:2204.05024](#); P. Asadi, C. Cesarotti, K. Fraser, S. Homiller, and A. Parikh, Oblique lessons from the W mass measurement at CDF II, [arXiv:2204.05283](#); P. Athron, M. Bach, D. H. J. Jacob, W. Kotlarski, D. Stöckinger, and A. Voigt, Precise calculation of the W boson pole mass beyond the Standard Model with FlexibleSUSY, [arXiv:2204.05285](#); K. Sakurai, F. Takahashi, and W. Yin, Singlet extensions and W boson mass in the light of the CDF II result, [arXiv:2204.04770](#); J. Fan, L. Li, T. Liu, and K. F. Lyu, W -boson mass, electroweak precision tests and SMEFT, [arXiv:2204.04805](#); X. Liu, S. Y. Guo, B. Zhu, and Y. Li, Unifying gravitational waves with W boson, FIMP dark matter, and Majorana Seesaw mechanism, [arXiv:2204.04834](#); G. Cacciapaglia and F. Sannino, The W boson mass weighs in on the non-standard Higgs, [arXiv:2204.04514](#); M. Blennow, P. Coloma, E. Fernández-Martínez, and M. González-López, Right-handed neutrinos and the CDF II anomaly, [arXiv:2204.04559](#); A. Strumia, Interpreting electroweak precision data including the W -mass CDF anomaly, [arXiv:2204.04191](#); C. R. Zhu, M. Y. Cui, Z. Q. Xia, Z. H. Yu, X. Huang, Q. Yuan, and Y. Z. Fan, GeV antiproton/gamma-ray excesses and the W -boson mass anomaly: Three faces of ~ 60 – 70 GeV dark matter particle?, [arXiv:2204.03767](#); P. Athron, A. Fowlie, C. T. Lu, L. Wu, Y. Wu, and B. Zhu, The W boson mass and muon $g-2$: Hadronic uncertainties or new physics?, [arXiv:2204.03996](#); J. M. Yang and Y. Zhang, Low energy SUSY confronted with new measurements of W -boson mass and muon $g-2$, [arXiv:2204.04202](#); J. de Blas, M. Pierini, L. Reina, and L. Silvestrini, Impact of the recent measurements of the top-quark and W -boson masses on electroweak precision fits, [arXiv:2204.04204](#); T. P. Tang, M. Abdughani, L. Feng, Y. L. S. Tsai, and Y. Z. Fan, NMSSM neutralino dark matter for W -boson mass and muon $g-2$ and the promising prospect of direct detection, [arXiv:2204.04356](#); X. K. Du, Z. Li, F. Wang, and Y. K. Zhang, Explaining the muon $g-2$ anomaly and new CDF II W -boson mass in the framework of (extra)ordinary gauge mediation, [arXiv:2204.04286](#); A. Batra, S. K. A. S. Mandal, and R. Srivastava, W boson mass in singlet-triplet scotogenic dark matter model, [arXiv:2204.09376](#); E. d. Almeida, A. Alves, O. J. P. Eboli, and M. C. Gonzalez-Garcia, Impact of CDF-II measurement of M_W on the electroweak legacy of the LHC Run II, [arXiv:2204.10130](#); Y. Cheng, X. G. He, F. Huang, J. Sun, and Z. P. Xing, Dark photon kinetic mixing effects for CDF W mass excess, [arXiv:2204.10156](#); J. Heeck, W -boson mass in the triplet seesaw model, [arXiv:2204.10274](#); A. Addazi, A. Marciano, R. Pasechnik, and H. Yang, CDF II W -mass anomaly faces first-order electroweak phase transition, [arXiv:2204.10315](#);
- [10] Y. Z. Fan, T. P. Tang, Y. L. S. Tsai, and L. Wu, Inert Higgs Dark Matter for New CDF W -boson Mass and Detection Prospects, *Phys. Rev. Lett.* **129**, 091802 (2022).
 - [11] B. Y. Zhu, S. Li, J. G. Cheng, R. L. Li, and Y. F. Liang, Using gamma-ray observation of dwarf spheroidal galaxy to test a dark matter model that can interpret the W -boson mass anomaly, [arXiv:2204.04688](#).
 - [12] H. Song, W. Su, and M. Zhang, Electroweak phase transition in 2HDM under Higgs, Z -pole, and W precision measurements, [arXiv:2204.05085](#).
 - [13] H. Bahl, J. Braathen, and G. Weiglein, New physics effects on the W -boson mass from a doublet extension of the SM Higgs sector, *Phys. Lett. B* **833**, 137295 (2022).
 - [14] K. S. Babu, S. Jana, and V. P. K., Correlating W -Boson Mass Shift with Muon $g-2$ in the 2HDM, *Phys. Rev. Lett.* **129**, 121803 (2022).
 - [15] Y. Heo, D. W. Jung, and J. S. Lee, Impact of the CDF W -mass anomaly on two Higgs doublet model, *Phys. Lett. B* **833**, 137274 (2022).
 - [16] O. Atkinson, M. Black, A. Lenz, A. Rusov, and J. Wynne, Cornering the two Higgs doublet model type II, *J. High Energy Phys.* **04** (2022) 172.
 - [17] O. Atkinson, M. Black, C. Englert, A. Lenz, A. Rusov, and J. Wynne, The flavourful present and future of 2HDMs at the collider energy frontier, [arXiv:2202.08807](#).
 - [18] F. J. Botella, F. Cornet-Gomez, and M. Nebot, Flavor conservation in two-Higgs-doublet models, *Phys. Rev. D* **98**, 035046 (2018).
 - [19] A. Broggio, E. J. Chun, M. Passera, K. M. Patel, and S. K. Vempati, Limiting two-Higgs-doublet models, *J. High Energy Phys.* **11** (2014) 058.

- [20] K. S. Kumar, S. Mantry, W. J. Marciano, and P. A. Souder, Low energy measurements of the weak mixing angle, *Annu. Rev. Nucl. Part. Sci.* **63**, 237 (2013).
- [21] C. T. Lu, L. Wu, Y. Wu, and B. Zhu, Electroweak precision fit and new physics in light of W boson mass, *Phys. Rev. D* **106**, 035034 (2022).
- [22] G. Kreyerhoff and R. Rodenberg, Renormalization group analysis of Coleman-Weinberg symmetry breaking in two Higgs models, *Phys. Lett. B* **226**, 323 (1989); J. Freund, G. Kreyerhoff, and R. Rodenberg, Vacuum stability in a two Higgs model, *Phys. Lett. B* **280**, 267 (1992); B. M. Kastening, Bounds from stability and symmetry breaking on parameters in the two Higgs doublet potential, [arXiv:hep-ph/9307224](https://arxiv.org/abs/hep-ph/9307224); S. Nie and M. Sher, Vacuum stability bounds in the two Higgs doublet model, *Phys. Lett. B* **449**, 89 (1999); S. Kanemura, T. Kasai, and Y. Okada, Mass bounds of the lightest CP even Higgs boson in the two Higgs doublet model, *Phys. Lett. B* **471**, 182 (1999).
- [23] P. M. Ferreira and D. R. T. Jones, Bounds on scalar masses in two Higgs doublet models, *J. High Energy Phys.* **08** (2009) 069.
- [24] H. A. Weldon, The effects of multiple Higgs bosons on tree unitarity, *Phys. Rev. D* **30**, 1547 (1984); S. Kanemura, T. Kubota, and E. Takasugi, Lee-Quigg-Thacker bounds for Higgs boson masses in a two doublet model, *Phys. Lett. B* **313**, 155 (1993); A. G. Akeroyd, A. Arhrib, and E.-M. Naimi, Note on tree level unitarity in the general two Higgs doublet model, *Phys. Lett. B* **490**, 119 (2000); I. F. Ginzburg and I. P. Ivanov, Tree-level unitarity constraints in the most general 2HDM, *Phys. Rev. D* **72**, 115010 (2005).
- [25] D. Eriksson, J. Rathsman, and O. Stal, 2HDMC: Two-Higgs-doublet model calculator physics and manual, *Comput. Phys. Commun.* **181**, 189 (2010).
- [26] M. Benedikt and F. Zimmermann, Future circular collider: Integrated programme and feasibility study, *Front. Phys.* **10**, 888078 (2022).
- [27] A. Blondel and P. Janot, FCC-ee overview: New opportunities create new challenges, *Eur. Phys. J. Plus* **137**, 92 (2022).
- [28] J. F. Gunion and H. E. Haber, The CP conserving two Higgs doublet model: The approach to the decoupling limit, *Phys. Rev. D* **67**, 075019 (2003).
- [29] S. Chang, S. K. Kang, J. P. Lee, K. Y. Lee, S. C. Park, and J. Song, Comprehensive study of two Higgs doublet model in light of the new boson with mass around 125 GeV, *J. High Energy Phys.* **05** (2013) 075.
- [30] G. C. Branco, P. M. Ferreira, L. Lavoura, M. N. Rebelo, M. Sher, and J. P. Silva, Theory and phenomenology of two-Higgs-doublet models, *Phys. Rep.* **516**, 1 (2012).
- [31] D. Toussaint, Renormalization effects From superheavy Higgs particles, *Phys. Rev. D* **18**, 1626 (1978).
- [32] S. Kanemura, Y. Okada, H. Taniguchi, and K. Tsumura, Indirect bounds on heavy scalar masses of the two-Higgs-doublet model in light of recent Higgs boson searches, *Phys. Lett. B* **704**, 303 (2011).
- [33] M. Baak, M. Goebel, J. Haller, A. Hoecker, D. Ludwig, K. Moenig, M. Schott, and J. Stelzer, Updated status of the global electroweak fit and constraints on new physics, *Eur. Phys. J. C* **72**, 2003 (2012).
- [34] H. E. Haber and D. O'Neil, Basis-independent methods for the two-Higgs-doublet model III: The CP -conserving limit, custodial symmetry, and the oblique parameters S , T , U , *Phys. Rev. D* **83**, 055017 (2011).
- [35] John F. Gunion, Howard E. Haber, Gordon Kane, and Sally Dawson, *The Higgs Hunter's Guide* (Addison-Wesley Publishing Company, Redwood City, California, 1990).
- [36] K. Cheung and O. C. W. Kong, Can the two Higgs doublet model survive the constraint from the muon anomalous magnetic moment as suggested?, *Phys. Rev. D* **68**, 053003 (2003).
- [37] P. H. Chankowski, M. Krawczyk, and J. Zochowski, Implications of the precision data for very light Higgs boson scenario in 2HDM(II), *Eur. Phys. J. C* **11**, 661 (1999).
- [38] A. Sopczak, Higgs physics: From LEP to a future linear collider, [arXiv:hep-ph/0502002](https://arxiv.org/abs/hep-ph/0502002).
- [39] S. Schael *et al.* (ALEPH and DELPHI and L3 and OPAL and LEP Working Group for Higgs Boson Searches Collaborations), Search for neutral MSSM Higgs bosons at LEP, *Eur. Phys. J. C* **47**, 547 (2006).
- [40] A. Heister *et al.* (ALEPH Collaboration), Search for charged Higgs bosons in e^+e^- collisions at energies up to $\sqrt{s} = 209$ -GeV, *Phys. Lett. B* **543**, 1 (2002).
- [41] T. V. Duong, E. Keith, E. Ma, and H. Kikuchi, Decay of Z into two light Higgs bosons, *Phys. Rev. D* **52**, 5045 (1995).
- [42] CMS Collaboration, Report No. CMS-PAS-HIG-13-026.
- [43] G. Aad *et al.* (ATLAS Collaboration), Search for charged Higgs bosons decaying via $H^\pm \rightarrow \tau^\pm \nu$ in fully hadronic final states using pp collision data at $\sqrt{s} = 8$ TeV with the ATLAS detector, *J. High Energy Phys.* **03** (2015) 088.
- [44] G. Aad *et al.* (ATLAS Collaboration), Search for charged Higgs bosons decaying via $H^\pm \rightarrow \tau^\pm \nu$ in fully hadronic final states using pp collision data at $\sqrt{s} = 8$ TeV with the ATLAS detector, *J. High Energy Phys.* **03** (2015) 088.
- [45] M. Misiak and M. Steinhauser, Weak radiative decays of the B meson and bounds on M_{H^\pm} in the Two-Higgs-Doublet Model, *Eur. Phys. J. C* **77**, 201 (2017).
- [46] A. Abdesselam *et al.* (Belle Collaboration), Measurement of the inclusive $B \rightarrow X_{s+d} \gamma$ branching fraction, photon energy spectrum and HQE parameters, [arXiv:1608.02344](https://arxiv.org/abs/1608.02344).
- [47] M. Misiak and M. Steinhauser, Weak radiative decays of the B meson and bounds on M_{H^\pm} in the Two-Higgs-Doublet Model, *Eur. Phys. J. C* **77**, 201 (2017).
- [48] P. M. Ferreira, H. E. Haber, R. Santos, and J. P. Silva, Mass-degenerate Higgs bosons at 125 GeV in the two-Higgs-doublet model, [arXiv:1211.3131](https://arxiv.org/abs/1211.3131).
- [49] S. K. Kang, Z. Qian, J. Song, and Y. W. Yoon, Confronting the fourth generation two Higgs doublet model with the phenomenology of heavy Higgs bosons, *Phys. Rev. D* **98**, 095025 (2018); T. Han, S. K. Kang, and J. Sayre, Muon $g-2$ in the aligned two Higgs doublet model, *J. High Energy Phys.* **02** (2016) 097; S. Chang, S. K. Kang, J. P. Lee, and J. Song, Higgs potential and hidden light Higgs scenario in two Higgs doublet models, *Phys. Rev. D* **92**, 075023 (2015); S. Chang, S. K. Kang, J. P. Lee, K. Y. Lee, S. C. Park, and J. Song, Two Higgs doublet models for the

- LHC Higgs boson data at $\sqrt{s} = 7$ and 8 TeV, *J. High Energy Phys.* **09** (2014) 101; H. S. Cheon and S. K. Kang, Constraining parameter space in type-II two-Higgs doublet model in light of a 126 GeV Higgs boson, *J. High Energy Phys.* **09** (2013) 085.
- [50] P. Bechtle, D. Dercks, S. Heinemeyer, T. Klingl, T. Stefaniak, G. Weiglein, and J. Wittbrodt, HiggsBounds-5: Testing Higgs sectors in the LHC 13 TeV Era, *Eur. Phys. J. C* **80**, 1211 (2020).
- [51] P. Bechtle, S. Heinemeyer, T. Klingl, T. Stefaniak, G. Weiglein, and J. Wittbrodt, HiggsSignals-2: Probing new physics with precision Higgs measurements in the LHC 13 TeV era, *Eur. Phys. J. C* **81**, 145 (2021).
- [52] F. Mahmoudi, SUPERISO v2.3: A program for calculating flavor physics observables in Supersymmetry, *Comput. Phys. Commun.* **180**, 1579 (2009).
- [53] D. Foreman-Mackey, D. W. Hogg, D. Lang, and J. Goodman, emcee: The MCMC Hammer, *Publ. Astron. Soc. Pac.* **125**, 306 (2013).
- [54] C. P. Burgess, S. Godfrey, H. Konig, D. London, and I. Maksymyk, A global fit to extended oblique parameters, *Phys. Lett. B* **326**, 276 (1994).
- [55] M. Ciuchini, E. Franco, S. Mishima, and L. Silvestrini, Electroweak precision observables, new physics and the nature of a 126 GeV Higgs boson, *J. High Energy Phys.* **08** (2013) 106.